Ecological Modelling 491 (2024) 110672

Contents lists available at ScienceDirect

Ecological Modelling

journal homepage: www.elsevier.com/locate/ecolmodel

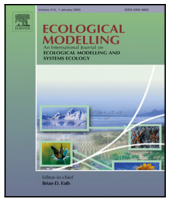

Fish survival subject to algal bloom: Resource-based growth models with algal digestion delay and detritus-nutrient recycling delay

Qi An [a], Hao Wang [b], Xiunan Wang [c,*]

[a] School of Mathematics and Statistics, Nanjing University of Information Science and Technology, Nanjing, Jiangsu 210044, China
[b] Department of Mathematical and Statistical Sciences, University of Alberta, Edmonton, AB T6G 2G1, Canada
[c] Department of Mathematics, University of Tennessee at Chattanooga, Chattanooga, TN 37403, USA

ARTICLE INFO

Keywords:
Algal bloom
Dissolved oxygen
Delay differential equations
Stability switch
Bifurcation

ABSTRACT

In this paper, we propose a class of resource-based growth models with delays in algal digestion and detritus-nutrient recycling, and investigate the model based on two different survival scenarios of algae during nutrient transformation. One scenario considers the survival rates of algae during nutrient uptake, while the other overlooks this factor. We find a significant difference in the estimated time window required for clearing the lake of detritus between the two models, and both are longer compared to the model without algal digestion delay. Moreover, the internal equilibria of both scenarios undergo an infinite number of stability switches, however, the key parameters leading to these stability switches differ. Notably, in the model accounting for algal death during nutrient uptake, there exists a safe zone where the stability of the internal equilibrium remains unaffected by the detritus-nutrient recycling delay, provided that the algal digestion delay falls within a suitable range. The findings derived from this study can provide valuable insights for the development of efficacious approaches in safeguarding the ecological integrity, managing algal blooms, facilitating sustainable fishery practices, and fostering favorable economic outcomes within the realm of water resources advancement.

1. Introduction

Algal bloom refers to the harmful ecological phenomenon caused by the massive reproduction and accumulation of phytoplankton in waterbodies. For example, the increase of dinoflagellate biomass may discolor the water and destroy the marine environment, which is often called red-tide disaster, while diatoms, most of which have spines, can clog and damage the gills of fish, leading to death (Kent et al., 1995; Sanseverino et al., 2016; Sellner et al., 2003). In fact, many algae can produce toxins, which will accumulate in shellfish and filter-feeding bivalves, seriously threatening the survival of the aquatic organisms. Consumption of these toxic aquatic products may cause damage to different systems of the human body, such as nervous and intestinal system (Christian and Luckas, 2008). In addition, in the late stage of the blooms, a large number of algae die and become debris under the action of bacterial decomposition. This process would consume a large amount of oxygen, which would lead to the anoxic death of marine organisms, resulting in the loss of fishery economy (Berdalet et al., 2016; Jeppesen et al., 2012). At present, blooms are occurring more frequently and have become a global disaster. There are many factors that affect the formation of algal bloom, such as appropriate temperature, high PH value, long time of light, low salinity and other natural conditions. Meanwhile, eutrophication of water and global warming caused by human activities also accelerate its occurrence. With the rapid development of modern chemical and agricultural production, a large amount of industrial and agricultural wastewater and domestic sewage is discharged into the sea, which leads to the increase of nutrients such as nitrogen and phosphorus, trace elements such as iron and manganese and organic compounds in the water, and promotes the mass reproduction of algae (Conley et al., 2009; William et al., 2008).

In recent decades, scientists have developed many ways to control and prevent blooms (Balaji-Prasath et al., 2022). The use of algaecides is one of the effective ways to mitigate and control harmful algal blooms, but due to its toxicity to other aquatic organisms, this method also has certain limitations (Anderson, 2009; Ebenezer et al., 2014; Grattan et al., 2016). There are also biological methods to kill algae directly or indirectly by using natural enemies and some microbial metabolites. These methods can ensure environmental safety but often take a long time to achieve inhibition, and it is difficult to cultivate a sufficient number of natural enemies, resulting in limited ecosystem-scale applications (Xiao et al., 2019; Zhang et al., 2018). In addition, ultrasonic vibrations, centrifugal separators and ultraviolet radiation can also be used to remove harmful algae, which are typically effective

* Corresponding author.
E-mail addresses: anqi@nuist.edu.cn (Q. An), hao8@ualberta.ca (H. Wang), xiunan-wang@utc.edu (X. Wang).

https://doi.org/10.1016/j.ecolmodel.2024.110672
Received 19 June 2023; Received in revised form 18 February 2024; Accepted 27 February 2024

for small blooms but come with higher costs (Alam et al., 2001; Dehghani, 2016). In general, the treatment of blooms has received great attention and each method has its advantages. Compared with governance methods, predicting the trend of nutrient load changes in response to water blooms, evaluating the impact of water blooms on ecosystems, and developing mitigation strategies are equally important for effectively preventing the occurrence of water blooms.

At present, many mathematical models have been developed to tease out the dynamics behind observations, simulate and predict algal bloom events, and reduce their impact on ecology and fishery economy (Jøorgensen, 1976; Voinov and Tonkikh, 1987; Wong et al., 2007). O'Brien (1974) proposed one of the first successful models to describe the dynamic characteristics of nutrient phytoplankton interactions, indicating that the mortality rate of phytoplankton is an important influence on the steady state nutrient concentration and population density. Huppert et al. (2005a,b) described the bottom-up nutrient phytoplankton models to help understand the dynamics of seasonally recurring algae blooms. Chen et al. (2015) established a nutrient phytoplankton model that combines the comprehensive effects of temperature and light, and proved that reducing nutrient load is an effective way to prevent the occurrence of algal bloom. A nonlinear model for the algal bloom in a lake caused by excessive nutrient flow in domestic drainage and farmland runoff, was studied by Shukla et al. (2008), shown that as the rate of the cumulative nutrient discharge increases, the equilibrium level of dissolved oxygen decreases, but algal population and detritus increases, which will ultimately lead to algal bloom and economic losses in the fish industry. Zhao et al. (2020) investigated a stochastic algal growth model with the explicit incorporation of season-dependent light and nutrient availability, obtaining the threshold for determining the persistence and extinction of algae.

Some models specifically address the impact of time delay on algal blooms. Mukhopadhyay et al. (1998) considered the maturity time of the new born cells and proposed a delay differential equation of plankton growth with competition and allelopathy. The model shows a stable limit cycle oscillation when the allelopathic effect is of a stimulatory nature. On the basis of Mukhopadhyay's model, Chen et al. (2007) analyzed a modified delay differential equation for the growth of n-species of plankton and obtained a set of delay-dependent condition which ensures the existence of at least one positive periodic solution of the system. Chattopadhyay et al. (2002) discussed a delayed phytoplankton–zooplankton model with toxic substances and explained the cyclic nature of blooms by analyzing three types of distribution of toxic substances. Misra et al. (2011) modified the model in Shukla et al. (2008) by increasing the delay in conversion of detritus into nutrients. They discovered the stable switching phenomenon of equilibrium and used time delay as a parameter to obtain the threshold for the possibility of large-scale fish population death.

The inclusion of time delays, such as the time delay from nutrient absorption to algal growth and the time delay from detritus conversion to nutrients, is crucial in algal modeling, akin to the predator maturation delay in predator–prey interactions (see, e.g., Wang et al., 2019). However, existing literature predominantly focuses on only one of these delays in the system. In light of this gap, our study aims to address this limitation by incorporating the digestion delay of algae into the model in Misra et al. (2011), resulting in the establishment of a class of resource-based algal growth models. We investigate the impact of these two delays on the system and simultaneously consider two scenarios, namely the presence or absence of algal death during nutrient transformation, with a particular focus on determining the optimal time window for detritus removal in a lake to ensure fish survival. Additionally, we explore the effects of controlling eutrophication on algae dynamics and fish survival, offering valuable insights and recommendations for algal bloom management.

The rest of the paper is organized as follows. In Section 2, we formulate the model with algal digestion delay and detritus-nutrient recycling delay, and introduce two different scenarios related to the mortality rate of algae in the process of nutrient transformation. In sections 3, we study the stability and bifurcation properties of the model, and present some simplified results of the degenerate model. In Section 4, we conduct numerical simulations for the two scenarios introduced in Section 2, respectively. Finally, we discuss the relationship between these two scenarios, compare them with existing results, and propose strategies for adapting to ensure fish survival in Section 5.

2. Mathematical models with two delays

Here, we consider a system with four variables, namely nutrient concentration $n(t)$, algal population density $a(t)$, detritus density $S(t)$ and dissolved oxygen concentration $C(t)$ in a lake. We make the following basic assumptions: (i) Nutrients from agriculture and industry are supplied to the water body at a constant accumulation rate q and deplete with the rate $\alpha_0 n(t)$ due to natural factors. (ii) The rate at which nutrients are lost through algae is directly proportional to the Monod interaction between the algae density and nutrient concentration, i.e., $\beta_1 na/(\beta_{12}+\beta_{11}n)$, where $\beta_1, \beta_{11}, \beta_{12}$ are the Monod constants, with β_1/β_{11} being the maximal growth rate and β_{12}/β_{11} the half-saturation coefficient. It takes an average of τ_2 time for nutrients to convert into algal biomass and the conversion rate is θ_1. (iii) The mortality rate of algae is $d \geq 0$ within the average nutrient transformation period τ_2, then the survival rate of algae during this process is $e^{-d\tau_2}$. (iv) The depletion of algae is jointly determined by natural death at the rate of $\alpha_1 a(t)$ and intraspecific competition described by $\beta_{10}a^2(t)$; (v) Detritus is formed by the death of algae at a production rate of $\pi_1\alpha_1 a(t)+\pi_2\beta_{10}a^2(t)$. It can be converted into nutrients through bacterial decomposition at a ratio of $\delta S(t)$. This process takes an average of τ_1 time to complete, and the proportionality constant for the formation of nutrients from detritus is π. (vi) The concentration of dissolved oxygen in water increases due to the exchange of oxygen between water and air at the rate of q_c and the photosynthesis of algae at the rate of $\lambda_{11}a(t)$, while decreases due to the natural factor at the rate of $\alpha_2 C(t)$ and decomposition of detritus by bacteria at the rate of $\delta_1 S(t)$. Then, we establish the following resource-based growth models with algal digestion delay and detritus-nutrient recycling delay:

$$\begin{cases} \dfrac{\mathrm{d}n(t)}{\mathrm{d}t} = q-\alpha_0 n(t)-\dfrac{\beta_1 n(t)a(t)}{\beta_{12}+\beta_{11}n(t)}+\pi\delta S(t-\tau_1), \\ \dfrac{\mathrm{d}a(t)}{\mathrm{d}t} = \dfrac{e^{-d\tau_2}\theta_1\beta_1 n(t-\tau_2)a(t-\tau_2)}{\beta_{12}+\beta_{11}n(t-\tau_2)}-\alpha_1 a(t)-\beta_{10}a^2(t), \\ \dfrac{\mathrm{d}S(t)}{\mathrm{d}t} = \pi_1\alpha_1 a(t)+\pi_2\beta_{10}a^2(t)-\delta S(t), \\ \dfrac{\mathrm{d}C(t)}{\mathrm{d}t} = q_c-\alpha_2 C(t)+\lambda_{11}a(t)-\delta_1 S(t), \end{cases} \tag{1}$$

where $n(\theta)=n^0>0$, $a(\theta)=a^0\geq 0$, $S(\theta)=S^0\geq 0$ for $\theta\in[-\tau,0]$, $\tau=\max\{\tau_1,\tau_2\}$, $C(0)=C^0>0$. The descriptions of all the variables and parameters are given in Table 1. To make the model reasonable, the conversion rates need to meet $0<\pi,\pi_1,\pi_2<1$. Meanwhile, since the growth rate of algae should be positive, it is assumed that $\theta_1\beta_1-\beta_{11}\alpha_1>0$.

In fact, the possibility of algal mortality during the absorption and digestion of nutrients may vary depending on the algae species and environmental factors. Therefore, in this article, we will consider two scenarios:

(1) No algal death during nutrient transformation process, i.e., $d=0$.
This is because some algae, such as diatoms, can maximize the utilization of nutrients by compressing and recycling nutrient containing vesicles (known as food vesicles), and they also have hard cell walls that provide a certain degree of protection for themselves, making them more adaptable to the environment (Sabater, 2009). Therefore, when the environment is relatively suitable, they are less likely to die in the process of

Table 1
Variables and parameters of model (1).

Variable or parameter	Description
$n(t)$	concentration of nutrients
$a(t)$	density of algae
$S(t)$	density of detritus
$C(t)$	concentration of dissolved oxygen in a lake
q	input rate of nutrients in a lake
α_0	natural loss rate of nutrients in a lake
β_1	Monod constant
β_{12}	Monod constant
β_{11}	Monod constant
π	proportionality constant for the formation of nutrients from detritus
δ	decomposition rate of detritus due to the bacterial pool
θ_1	proportional coefficient of algal growth rate
τ_1	detritus-nutrient recycling delay
τ_2	delay from nutrient uptake to algae growth
α_1	natural death rate of algae
β_{10}	death rate due to crowding of algae with respect to the aquatic habitat
π_1	proportional constant of production rate of detritus due to natural death of algae
π_2	proportional constant of production rate of detritus due to intraspecific competition of algae
q_c	growth rate of dissolved oxygen through surface re-aeration
α_2	natural depletion rate of dissolved oxygen in a lake
λ_{11}	growth rate of dissolved oxygen due to photosynthesis by algae
δ_1	depletion rate of dissolved oxygen by transformation of detritus into nutrients
d	average death rate of algea in the process of nutrient uptake and growth

absorbing and digesting nutrients. In this case, we can assume that the nutrients absorbed by algae are completely converted into their biomass, and take $d = 0$, then model (1) will degenerate into a two-delay model with delay-independent parameters. We will refer to the model corresponding to this situation as a degenerate model.

(2) Incorporating algal mortality during nutrient transformation process, i.e., $d > 0$.
In addition to the species of algae, environmental factors also have a significant impact on the growth and metabolism of algae. Under some harsh conditions, such as rapid or significant temperature changes, the cell membrane structure of algae can be disrupted, affecting the synthesis of intracellular proteins and the transportation of active enzymes and nutrients, resulting in the death of algae in the process of absorbing and digesting nutrients (Zachleder et al., 2016). Therefore, in this case, we need to consider the mortality of algae during the nutrient transformation process, which requires the parameter to meet $d > 0$. Then model (1) is actually a two-delay model with delay-dependent parameters, and we call it the non-degenerate model.

As we will see below, there are significant differences between the two scenarios for determining the optimal time window for removing lake debris.

3. Dynamic analysis for the algal growth model

In this section, we will discuss the stability and bifurcation of model (1), and these results are applicable to both degenerate and non-degenerate models. Comparing the two models, the degenerate model is a model with coefficients independent of time delay, and the corresponding analysis will be more concise. We will summarize some simplified results about the degenerate model at the end of this section.

3.1. Equilibrium analysis

The model (1) has two non-negative equilibria. One is the trivial equilibrium $\mathcal{E}_0(q/\alpha_0, 0, 0, q_c/\alpha_2)$, which always exists, and the other is the interior equilibrium $\mathcal{E}_1(n_0, a_0, S_0, C_0)$, which exists under the following conditions:

(H1) $(e^{-d\tau_2}\theta_1\beta_1 - \beta_{11}\alpha_1)q - \beta_{12}\alpha_0\alpha_1 > 0, \quad q_c + \lambda_{11}a_0 - \delta_1 S_0 > 0.$

Here $a_0 \in \left(0, (e^{-d\tau_2}\theta_1\beta_1 - \beta_{11}\alpha_1)/\beta_{10}\beta_{11}\right)$ is the zero of the following function:

$$G(a) = \left[(\pi\pi_2 - \frac{1}{e^{-d\tau_2}\theta_1})\beta_{10}a^2 + (\pi\pi_1 - \frac{1}{e^{-d\tau_2}\theta_1})\alpha_1 a + q\right] \times [(e^{-d\tau_2}\theta_1\beta_1 - \beta_{11}\alpha_1) - \beta_{10}\beta_{11}a] - \beta_{12}\alpha_0(\alpha_1 + \beta_{10}a), \tag{2}$$

and

$$n_0 = \beta_{12}(\alpha_1 + \beta_{10}a_0)/[(e^{-d\tau_2}\theta_1\beta_1 - \beta_{11}\alpha_1) - \beta_{10}\beta_{11}a_0],$$
$$S_0 = \frac{\pi_1\alpha_1 a_0 + \pi_2\beta_{10}a_0^2}{\delta},$$
$$C_0 = \frac{1}{\alpha_2}(q_c + \lambda_{11}a_0 - \delta_1 S_0).$$

We can notice that when $d > 0$, the interior equilibrium $\mathcal{E}_1$ depends on the algae digestion delay τ_2, and exists only when τ_2 is not too large, which is in line with the biological law that the average life cycle of general algae is not long. In addition, when $\tau_2 = 0$ or $d = 0$, the nontrivial equilibrium $\mathcal{E}_1$ degenerates to the case without time delays (Shukla et al., 2008). For the sake of subsequent analysis, we denote $\mathcal{E}_1(n_0, a_0, S_0, C_0)$ by $\mathcal{E}_1(n_0(\tau_2), a_0(\tau_2), S_0(\tau_2), C_0(\tau_2))$.

3.2. Bifurcation analysis

The stability of these two non-negative equilibria for $(\tau_1, \tau_2) = (0, 0)$ have been studied in Shukla et al. (2008), as stated in the following lemma:

Lemma 3.1. *(Shukla et al., 2008) Assume that (H1) holds, then for $(\tau_1, \tau_2) = (0, 0)$, the boundary equilibrium $\mathcal{E}_0$ is unstable and the internal equilibrium $\mathcal{E}_1$ is locally asymptotically stable.*

Next, we will study the influence of the two delays (τ_1, τ_2) on the stability of $\mathcal{E}_1$. Linearizing model (1) at $\mathcal{E}_1$ yields the following linear system:

$$\frac{d}{dt}v(t) = \mathcal{A}v(t) + \mathcal{B}v(t - \tau_1) + Cv(t - \tau_2), \tag{3}$$

where $v(t) = (n(t), a(t), S(t), C(t))^T$,

$$\mathcal{A} = \begin{pmatrix} -\alpha_0 - \frac{\beta_1\beta_{12}a_0}{(\beta_{12}+\beta_{11}n_0)^2} & -\frac{\beta_1 n_0}{\beta_{12}+\beta_{11}n_0} & 0 & 0 \\ 0 & -\alpha_1 - 2\beta_{10}a_0 & 0 & 0 \\ 0 & \pi_1\alpha_1 + 2\pi_2\beta_{10}a_0 & -\delta & 0 \\ 0 & \lambda_{11} & -\delta_1 & -\alpha_2 \end{pmatrix},$$

$$\mathcal{B}=\begin{pmatrix}0&0&\pi\delta&0\\0&0&0&0\\0&0&0&0\\0&0&0&0\end{pmatrix},\quad \mathcal{C}=\begin{pmatrix}0&0&0&0\\\frac{e^{-d\tau_2}\theta_1\beta_1\beta_{12}a_0}{(\beta_{12}+\beta_{11}n_0)^2}&\frac{e^{-d\tau_2}\theta_1\beta_1 n_0}{\beta_{12}+\beta_{11}n_0}&0&0\\0&0&0&0\\0&0&0&0\\0&0&0&0\end{pmatrix}.$$

The characteristic equation of (3) is a transcendental equation with delay dependent parameters:

$$(\lambda+\alpha_2)[P_0(\lambda,\tau_2)+P_1(\lambda,\tau_2)e^{-\lambda\tau_2}+P_2(\lambda,\tau_2)e^{-\lambda(\tau_1+\tau_2)}]=0, \tag{4}$$

where

$$P_0(\lambda,\tau_2)=\lambda^3+b_1\lambda^2+b_2\lambda+b_3,$$
$$P_1(\lambda,\tau_2)=-\frac{e^{-d\tau_2}\theta_1\beta_1 n_0}{\beta_{12}+\beta_{11}n_0}[\lambda^2+(\delta+\alpha_0)\lambda+\delta\alpha_0],$$
$$P_2(\lambda,\tau_2)=-\frac{e^{-d\tau_2}\pi\delta\theta_1\beta_1\beta_{12}a_0}{(\beta_{12}+\beta_{11}n_0)^2}(\pi_1\alpha_1+2\pi_2\beta_{10}a_0),$$

with

$$b_1=\delta+\alpha_0+\alpha_1+2\beta_{10}a_0+\frac{\beta_1\beta_{12}a_0}{(\beta_{12}+\beta_{11}n_0)^2},$$
$$b_2=\Big[\alpha_0+\frac{\beta_1\beta_{12}a_0}{(\beta_{12}+\beta_{11}n_0)^2}\Big](\alpha_1+2\beta_{10}a_0)+\delta\Big[\alpha_0+\alpha_1+2\beta_{10}a_0+\frac{\beta_1\beta_{12}a_0}{(\beta_{12}+\beta_{11}n_0)^2}\Big],$$
$$b_3=\delta\Big[\alpha_0+\frac{\beta_1\beta_{12}a_0}{(\beta_{12}+\beta_{11}n_0)^2}\Big](\alpha_1+2\beta_{10}a_0).$$

It is easy to see that $\lambda=-\alpha_2<0$ is one root of (4), and the other roots satisfy

$$D(\lambda;\tau_1,\tau_2)\equiv P_0(\lambda,\tau_2)+P_1(\lambda,\tau_2)e^{-\lambda\tau_2}+P_2(\lambda,\tau_2)e^{-\lambda(\tau_1+\tau_2)}=0. \tag{5}$$

Note that all the characteristic roots of (5) have negative real parts for $(\tau_1,\tau_2)=(0,0)$, and the stability of $\mathcal{E}_1$ changes only if a characteristic root appears on or crosses the imaginary axis. So we are going to find the purely imaginary characteristic roots of (5). Substituting $\lambda=i\omega$ into (5), we have that $D(i\omega;\tau_1,\tau_2)=0$ if and only if

$$1+a_1(\omega,\tau_2)e^{-i\omega\tau_2}+a_2(\omega,\tau_2)e^{-i\omega(\tau_1+\tau_2)}=0 \tag{6}$$

where

$$a_j(\omega,\tau_2)=P_j(i\omega,\tau_2)/P_0(i\omega,\tau_2),\ \ j=1,2.$$

According to the geometric method proposed in An et al. (2019), Gu et al. (2005), Lin and Wang (2012), we consider the three terms 1, $a_1(\omega,\tau_2)e^{-\lambda\tau_2}$ and $a_2(\omega,\tau_2)e^{-\lambda(\tau_1+\tau_2)}$, as three vectors in complex plane, with the magnitudes 1, $|a_1(\omega,\tau_2)|$ and $|a_2(\omega,\tau_2)|$, respectively. Then, any solution of (6) must put these vectors connect to each other and form a triangle, form which we have the following lemma for the feasible region of (ω,τ_2).

Lemma 3.2. *For $\omega>0$, $(i\omega,\tau_1,\tau_2)$ can be the zero of (5) only if (ω,τ_2) satisfies*

$$\begin{aligned}F_1(\omega,\tau_2)&:=|P_0(i\omega,\tau_2)|+|P_1(i\omega,\tau_2)|-|P_2(i\omega,\tau_2)|\geq 0,\\F_2(\omega,\tau_2)&:=|P_0(i\omega,\tau_2)|+|P_2(i\omega,\tau_2)|-|P_1(i\omega,\tau_2)|\geq 0,\\F_3(\omega,\tau_2)&:=|P_1(i\omega,\tau_2)|+|P_2(i\omega,\tau_2)|-|P_0(i\omega,\tau_2)|\geq 0.\end{aligned} \tag{7}$$

We use Ω to represent the set of all the points $(\omega,\tau_2)\in\mathbb{R}^2_+$ that meet the inequalities (7). Note that Ω may consist of multiple simply connected regions Ω_k, $k=1,2,\dots,N$. For each Ω_k, the admissible range for ω is denoted by I_k, $k=1,2,\dots,N$. According to the relationship of these three vectors 1, $a_1(\omega,\tau_2)e^{-\lambda\tau_2}$ and $a_2(\omega,\tau_2)e^{-\lambda(\tau_1+\tau_2)}$, the solution $(i\omega,\tau_1,\tau_2)$ of (5) must satisfy

$$\arg(a_1(\omega,\tau_2)e^{-i\omega\tau_2})=\pi-\theta_1(\omega,\tau_2),$$
$$\arg(a_2(\omega,\tau_2)e^{-i\omega(\tau_1+\tau_2)})=\theta_2(\omega,\tau_2)-\pi,\qquad(\omega,\tau_2)\in\Omega$$

or

$$\arg(a_1(\omega,\tau_2)e^{-i\omega\tau_2})=\theta_1(\omega,\tau_2)-\pi,$$
$$\arg(a_2(\omega,\tau_2)e^{-i\omega(\tau_1+\tau_2)})=\pi-\theta_2(\omega,\tau_2),\qquad(\omega,\tau_2)\in\Omega$$

where $\theta_1(\omega,\tau_2)$, $\theta_2(\omega,\tau_2)$ are the angles formed by 1 and $a_1(\omega,\tau_2)e^{-i\omega\tau_2}$, 1 and $a_2(\omega,\tau_2)e^{-i\omega(\tau_1+\tau_2)}$, respectively, given by the following formula:

$$\theta_1(\omega,\tau_2)=\arccos\left(\frac{1+|a_1(\omega,\tau_2)|^2-|a_2(\omega,\tau_2)|^2}{2|a_1(\omega,\tau_2)|}\right),$$
$$\theta_2(\omega,\tau_2)=\arccos\left(\frac{1+|a_2(\omega,\tau_2)|^2-|a_1(\omega,\tau_2)|^2}{2|a_2(\omega,\tau_2)|}\right).$$

Then, we can first solve $(\omega,\tau_2)\in\Omega$ by finding the zeros of the following implicit function:

$$S_n^{\pm}(\omega,\tau_2)=\tau_2-\frac{1}{\omega}[\arg(a_1(\omega,\tau_2))\pm\theta_1(\omega,\tau_2)+(2n-1)\pi],\quad n\in\mathbb{Z}. \tag{8}$$

Some numerical methods are required to solve the above equations. The zeros of (8), if they exist, are denoted by $(\omega,\tau_2^{n\pm}(\omega))$. The corresponding critical values of τ_1 can be set up by

$$\tau_1^{m,n\pm}(\omega)=\frac{1}{\omega}[\arg(a_2(\omega,\tau_2^{n\pm}(\omega)))\mp\theta_2(\omega,\tau_2^{n\pm}(\omega))+(2m+1)\pi]-\tau_2^{n\pm}(\omega),\quad m\geq m_0^{\pm}, \tag{9}$$

where $m_0^{\pm}$ is the smallest integer such that $\tau_1^{m,n\pm}(\omega)>0$.

Generally, calculating the root of Eq. (8) requires temporarily fixing ω, as ω takes the values throughout the interval I_k, $k=1,2,\dots,N$, and we can get the curve

$$\mathcal{C}:=\{(\omega,\tau_2^{n\pm}(\omega))\mid\omega\in I_k\ (k=1,\dots,N),\ S_n^{\pm}(\omega,\tau_2^{n\pm}(\omega))=0\} \tag{10}$$

on Ω, which will later determine the shape of the crossing curves

$$\mathcal{T}:=\{(\tau_1^{m,n\pm}(\omega),\tau_2^{n\pm}(\omega))\in\mathbb{R}^2_+\mid\omega\in I_k,\ k=1,2,\dots,N.\} \tag{11}$$

on (τ_1,τ_2)-plane.

We obtain the following conclusion about the existence of pure imaginary eigenvalues of Eq. (4).

Theorem 3.3. *Assume that $(H1)$ holds. Then the characteristic equation (4) admits a pair of conjugate roots $\lambda=\pm i\omega$ if and only if $\omega\in I_k$, $k=1,2,\dots,N$, and $(\tau_1,\tau_2)=(\tau_1^{m,n\pm}(\omega),\tau_2^{n\pm}(\omega))\in\mathcal{T}$.*

3.3. Crossing directions

All the points in $\mathcal{T}$ will form several continuous curves in $\tau_1-\tau_2$ plane, we call them the crossing curves (which are also the bifurcation curves under some suitable conditions). In this section, we will study the variation of the pure imaginary eigenvalues of (4) with the time delay (τ_1,τ_2), that is, calculate the crossing direction of the crossing curve. Assume that $(\tau_1^*,\tau_2^*)\in\mathcal{T}$, then there is a $\omega^*>0$ such that $(i\omega^*,\tau_1^*,\tau_2^*)$ solved the characteristic equation (4). If $\frac{\partial D}{\partial\lambda}(i\omega^*,\tau_1^*,\tau_2^*)\neq 0$, based on the implicit function theorem, the characteristic root λ can be considered as a function of (τ_1,τ_2) in the neighborhood of (τ_1^*,τ_2^*). Let $\lambda(\tau_1,\tau_2)=\alpha(\tau_1,\tau_2)+i\beta(\tau_1,\tau_2)$, which satisfies $\alpha(\tau_1^*,\tau_2^*)=0$ and $\beta(\tau_1^*,\tau_2^*)=\omega^*$. Next, we will discuss the directional derivatives of $\alpha(\tau_1,\tau_2)$ with respect to (τ_1,τ_2). As in An et al. (2019), Gu et al. (2005), we call the direction of the crossing curve $\mathcal{T}$ that corresponds to increasing ω the positive direction, and the region on the left-hand (right-hand) side when we move along the positive direction of the curve the region on the left (right).

Theorem 3.4. *Assume that $(i\omega^*,\tau_1^*,\tau_2^*)$ is a zero of (4) and satisfies $\frac{\partial D}{\partial\lambda}(i\omega^*,\tau_1^*,\tau_2^*)\neq 0$. Then as (τ_1,τ_2) passes through (τ_1^*,τ_2^*) from the region on the left to the region on the right of the crossing curves, the characteristic root $\lambda(\tau_1,\tau_2)$ crosses the imaginary axis from left to right whenever*

$$\delta(\tau_1^*,\tau_2^*)=\mathrm{Im}\{(-\omega^*+di)[\overline{P_2(\omega^*,\tau_2^*)}P_1(\omega^*,\tau_2^*)e^{i\omega^*\tau_1^*}]\}+d|P_2(\omega^*,\tau_2^*)|^2>0. \tag{12}$$

The crossing is in the opposite direction if the inequality is reversed.

Proof. A careful calculation gives that

$$\begin{aligned}\frac{\partial D}{\partial \tau_1}(i\omega^*,\tau_1^*,\tau_2^*) &= -i\omega^* P_2(i\omega^*,\tau_2^*)e^{-i\omega^*(\tau_1^*+\tau_2^*)},\\ \frac{\partial D}{\partial \tau_2}(i\omega^*,\tau_1^*,\tau_2^*) &= \frac{\partial P_1}{\partial \tau_2}(i\omega^*,\tau_2^*)e^{-i\omega^*\tau_2^*} - i\omega P_1(i\omega^*,\tau_2^*)e^{-i\omega^*\tau_2^*}\\ &\quad + \frac{\partial P_2}{\partial \tau_2}(i\omega^*,\tau_2^*)e^{-i\omega^*(\tau_1^*+\tau_2^*)} + i\omega^* P_2(i\omega^*,\tau_2^*)e^{-i\omega^*(\tau_1^*+\tau_2^*)}\\ &= -(d+i\omega^*)[P_1(i\omega^*,\tau_2^*)e^{-i\omega^*\tau_2^*} + P_2(i\omega^*,\tau_2^*)e^{-i\omega^*(\tau_1^*+\tau_2^*)}],\end{aligned}$$

Then, according to the method proposed in An et al. (2019), Gu et al. (2005), we have

$$\begin{aligned}&\mathrm{Sgn}\left\{\left(\frac{\partial\alpha}{\partial\tau_1},\frac{\partial\alpha}{\partial\tau_2}\right)\cdot\left(\frac{\partial\tau_2}{\partial\beta},-\frac{\partial\tau_1}{\partial\beta}\right)\Big|_{(\tau_1,\tau_2)=(\tau_1^*,\tau_2^*)}\right\}\\ =\ &\mathrm{Sgn}\left\{-\mathrm{Im}\left(\frac{\partial\overline{D}}{\partial\tau_1}\cdot\frac{\partial D}{\partial\tau_2}\right)\Big|_{(\tau_1,\tau_2)=(\tau_1^*,\tau_2^*)}\right\}\\ =\ &\mathrm{Sgn}\left\{(-\omega+di)\left(\overline{P_2(\omega^*,\tau_2^*)}P_1(\omega^*,\tau_2^*)e^{i\omega^*\tau_1^*}+|P_2(\omega^*,\tau_2^*)|^2\right)\right\}\\ =\ &\mathrm{Sgn}\left\{\mathrm{Im}\{(-\omega^*+di)[\overline{P_2(\omega^*,\tau_2^*)}P_1(\omega^*,\tau_2^*)e^{i\omega^*\tau_1^*}]\}+d|P_2(\omega^*,\tau_2^*)|^2\right\}\end{aligned}$$

from which we completed the proof. □

3.4. Some simplified results for the degenerate model

For model (1), we mainly consider two cases: $d = 0$ and $d > 0$, as mentioned in Section 2. For the case $d = 0$, which means that there is no algal death during the nutrient transformation process, it can be regarded as a degenerate form of model (1), and the corresponding dynamic analysis will be simpler. We list some simplified results for the case $d = 0$ as follows:

(1) When $d = 0$, the interior equilibrium can be obtained by taking $\tau_2 = 0$ in (2), i.e., $\mathcal{E}_1(n_0, a_0, S_0, C_0) = \mathcal{E}_1(n_0(0), a_0(0), S_0(0), C_0(0))$, which is consistent with the model without time delays in Shukla et al. (2008).

(2) The characteristic equation of (3) for the case $d = 0$ reduces to a transcendental equation with coefficients independent of delay. More precisely, $\lambda = i\omega$ is a characteristic root if and only if

$$D(i\omega,\tau_1,\tau_2) \equiv P_0(i\omega,0) + P_1(i\omega,0)e^{-i\omega\tau_2} + P_2(i\omega,0)e^{-i\omega(\tau_1+\tau_2)} = 0, \tag{13}$$

or

$$1 + a_1(\omega,0)e^{-i\omega\tau_2} + a_2(\omega,0)e^{-i\omega(\tau_1+\tau_2)} = 0.$$

(3) For the degenerate case with zero algal mortality rate, we only need to first determine the feasible region of ω by setting $\tau_2 = 0$ in the inequalities (7), instead of determining the two-dimensional region of (ω, τ_2) in Lemma 3.2 as for the non-degenerate case. In general, the feasible domain with respect to ω for $d = 0$ is an open interval, which can be denoted by I for brevity.

(4) After calculating the feasible region of ω, we can obtain the following explicit expressions for (τ_1, τ_2) with respect to ω, such that $(\omega, \tau_1, \tau_2) \in I \times \mathbb{R}^2_+$ solves Eq. (13):

$$\begin{aligned}\tau_2 = \tau_2^{n\pm}(\omega) &= \frac{1}{\omega}\left[\arg(a_1(\omega)) \pm \theta_1(\omega) + (2n-1)\pi\right], \quad n \in \mathrm{Z}, n \geq n_0^{\pm},\\ \tau_1 = \tau_1^{m,n\pm}(\omega) &= \frac{1}{\omega}\left[\arg(a_2(\omega)) \mp \theta_2(\omega) + (2m-1)\pi\right] - \tau_2^{n\pm}(\omega), \quad m \in \mathrm{Z}, m \geq m_0^{\pm},\end{aligned} \tag{14}$$

where $n_0^{\pm}, m_0^{\pm} \in \mathrm{Z}$ are the smallest possible integers that make $\tau_1^{m,n\pm}, \tau_2^{n\pm}$ nonnegative. This is different from the non-degenerate case, where the expression for τ_2 can only be given implicitly by (8), and also means that for the degenerate case, we do not need to draw the curve C as in (10), but can directly obtain the crossing curve $\mathcal{T}$ by tracing the point.

(5) For the case $d = 0$, the expression (12) in Theorem 3.4 to determine the crossing direction can be reduced to

$$\delta(\tau_1^*,\tau_2^*) = -\omega^*\mathrm{Im}\{\omega^*[\overline{P_2(\omega^*,0)}P_1(\omega^*,0)e^{i\omega^*\tau_1^*}]\} > 0. \tag{15}$$

Table 2
Parameter values in model (1).

Parameter	Value of parameter	Parameter	Value of parameter
q	0.5 mg l^{-1}day^{-1}	β_{10}	0.00001 1 mg^{-1}day^{-1}
α_0	0.005 day^{-1}	π_1	0.9
β_1	0.006 day^{-1}	π_2	0.5
β_{12}	5 mg l^{-1}	δ	0.1 day^{-1}
β_{11}	1	q_c	1 mg l^{-1}day^{-1}
π	0.02	α_2	0.05 day^{-1}
θ_1	50	λ_{11}	0.01 day^{-1}
α_1	0.25 day^{-1}	δ_1	0.0044 day^{-1}

4. Numerical simulation

In order to verify the rationality of the previous theoretical analysis, compare the dynamic behavior of model (1) with that of the model with a single detritus-nutrient recycling delay, and explore the impact of algal death during nutrient conversion on ecology, we will conduct numerical simulations for the case of $d = 0$ and $d > 0$ respectively in this section. The values of the parameters except the two delays and the algae mortality d are taken from Amemiyaa et al. (2007), Misra et al. (2011) and the references therein (see Table 2).

4.1. Numerical simulation of the degenerate model

We first consider the situation where algae do not die during the process of nutrient transformation, i.e. $d = 0$. Under the parameter values in the Table 2, the interior equilibrium $\mathcal{E}_1(n_0, a_0, S_0, C_0)$ of model (1) exists, and is given by $n_0 = 29.31$ mg l^{-1}, $a_0 = 628.02$ mg l^{-1}, $S_0 = 1432.77$ mg l^{-1}, $C_0 = 19.52$ mg l^{-1}. By solving the inequalities (7) with $\tau_2 = 0$, we can obtain that the feasible region for ω is $I = (0.0375, 0.0950)$. For each $\omega \in I$, one can calculate $(\tau_1^{m,n\pm}(\omega), \tau_2^{n\pm}(\omega)) \in \mathbb{R}^2_+$ by (14), for some suitable $n, m \in \mathbb{Z}$. Then the crossing curves (bifurcation curves)

$$\mathcal{T} = \{(\tau_1^{m,n\pm}(\omega), \tau_2^{n\pm}(\omega)) \in \mathbb{R}^2_+ \mid \omega \in I,\ n \geq n_0^{\pm},\ m \geq m_0^{\pm}\}$$

are obtained. Finally, the crossing direction for each $(\tau_1, \tau_2) \in T$ can be given by (15). We show the crossing curves and the crossing directions in Fig. 1, where the characteristic root $\lambda(\tau_1, \tau_2)$ will cross the imaginary axis from left to right if (τ_1, τ_2) is moving in the direction of the arrows.

By comparing the degenerate case of model (1) with the model that only considers the detritus-nutrient recycling delay τ_1 in Misra et al. (2011), the following conclusions can be drawn:

(1) If we ignore the delay from nutrient uptake to algae growth (i.e., $\tau_2 = 0$), the first critical value of the detritus-nutrient recycling delay $\tau_1 = 42$, which is consistent with the result obtained in Misra et al. (2011). See Fig. 1 for details. This implies that when the time delay τ_1 exceeds 42 days, there can be fluctuations in the concentration of dissolved oxygen. In certain instances, the concentration of dissolved oxygen may sharply decrease, leading to a significant mortality of the fish population in the lake. Consequently, these findings highlight the importance of timely detritus removal from the lake to prevent the occurrence of mass fish fatalities, particularly before the 42-day threshold.

Table 3
First critical value τ_1 for different τ_2.

τ_2 (days)	0	1	3	5	7	9
First critical value of τ_1 (days)	42	45	51.89	58.77	65.5	71.9

Table 4
First critical value τ_1 for different q when $\tau_2 = 5$.

q (mg l^{-1}day^{-1})	0.3	0.5	0.7	0.9	1.1	1.3	1.5	1.7
τ_2 (days)	5	5	5	5	5	5	5	5
First critical value of τ_1(days)	77	58.77	53.00	50.97	50.31	50.70	51.70	53.27
n^* (mg l^{-1})	26.99	29.31	31.72	34.26	36.95	39.83	42.93	46.29
a^* (mg l^{-1})	310.80	628.02	915.25	1179.27	1424.58	1654.31	1870.73	2075.53
S^* (mg l^{-1})	704.12	1432.77	2101.19	2722.89	3306.78	3859.04	4384.12	4885.32
C^* (mg l^{-1})	20.20	19.52	18.14	16.24	13.92	11.27	8.34	5.20

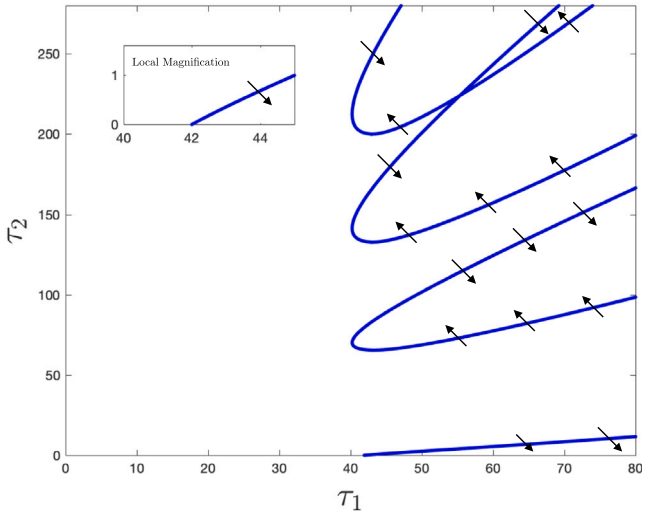

Fig. 1. Crossing curves and crossing directions.

(2) The time window for removal of detritus in a lake in order to guarantee the survival of fish will be underestimated if we ignore the delay from nutrient absorption to algal growth. Table 3 shows the changes of the first critical value τ_1 with the value of τ_2. For instance, when $\tau_2 = 5$, we can see that the corresponding critical value $\tau_1 = 58.77 > 42$. The solutions of model (1) with $d = 0$ shown in Fig. 2 verify this point, that is, E_1 is stable for $(\tau_1, \tau_2) = (52, 5)$ and unstable for $(\tau_1, \tau_2) = (65, 5)$, while a stable periodic solution bifurcated from E_1.

(3) As shown in Table 4, when the nutrient concentration q increases, the algae population will intensify, accompanied by a decline in the dissolved oxygen concentration in the water, resulting in a gradual reduction in fish density. This implies that an increase in water eutrophication will expedite the occurrence of algae blooms, leading to significant harm to the ecological environment and posing a threat to the growth of fisheries. Therefore, from both the environmental and economic perspectives, it is imperative to control eutrophication.

(4) By observing the crossing curves, we find that τ_2 can cause the stability switching of model (1) for the degenerate case. For instance, the stability of the interior equilibrium E_1 switches from unstable to stable to unstable, as (τ_1, τ_2) changes from $(65, 5)$ to $(65, 50)$ to $(65, 90)$. See Figs. 2 and 3 for details. This indicates that the system stability hinges upon a favorable range of the algal digestion delay τ_2 that should not be excessively high or low. This can be regulated by manipulating external environmental factors such as temperature or pH value.

4.2. Numerical simulation of the non-degenerate model

Now we consider the presence of algal death during nutrient conversion. The theoretical analysis in Section 3 shows that the non-degenerate case is much more difficult than the degenerate case in determining the bifurcation points due to the presence of the delay-dependent parameters. For many calculations, such as the feasible region Ω for (ω, τ_2) and the exact value of τ_2, numerical methods are required in this subsection. Therefore, in order to compare the dynamic behaviors between these two situations, we will do some numerical simulations on model (1) for $d > 0$. Let the average death rate $d = 0.1$ and the other parameter values except the two delays are the same as those in Table 2. Now the interior equilibrium $\mathcal{E}_1(n_0, a_0, S_0, C_0)$ depends on the value of τ_2. Specifically, $a_0 = a_0(\tau_2)$ is the zeros of the function $G(a)$. It can be observed that $G(a)$ is a cubic function of the variable a, so the display expression of $a_0 = a_0(\tau_2)$ cannot be given directly. However, due to the need of subsequent calculation, we must find the specific functional relationship between a_0 and τ_2. Therefore, here we shall make an approximation to the implicit function $a_0 = a_0(\tau_2)$.

Note that the value of $\beta_{10} = 0.00001$ is sufficiently small, then by comparing the coefficients, it can be found that the coefficient of the cubic term $-(\pi\pi_2 - \frac{1}{e^{-d\tau_2}\theta_1})\beta_{10}^2\beta_{11}$ in $G(a)$ is also sufficiently small, so we ignore the cubic term. Define

$$\tilde{a}_0(\tau_2) = \frac{-h_2(\tau_2) - \sqrt{h_2(\tau_2)^2 - 4h_1(\tau_2)h_3(\tau_2)}}{2h_1(\tau_2)} < \frac{e^{-d\tau_2}\theta_1\beta_1 - \beta_{11}\alpha_1}{\beta_{10}\beta_{11}}$$

where

$$h_1(\tau_2) = (e^{-d\tau_2}\theta_1\beta_1 - \beta_{11}\alpha_1)(\pi\pi_2 - \frac{1}{e^{-d\tau_2}\theta_1})\beta_{10} - \beta_{10}\beta_{11}(\pi\pi_1 - \frac{1}{e^{-d\tau_2}\theta_1})\alpha_1,$$

$$h_2(\tau_2) = (e^{-d\tau_2}\theta_1\beta_1 - \beta_{11}\alpha_1)(\pi\pi_1 - \frac{1}{e^{-d\tau_2}\theta_1})\alpha_1 - q\beta_{10}\beta_{11} - \beta_{12}\alpha_0\beta_{10},$$

$$h_3(\tau_2) = q(e^{-d\tau_2}\theta_1\beta_1 - \beta_{11}\alpha_1) - \beta_{12}\alpha_0\alpha_1.$$

Then the function $a_0 = \tilde{a}_0(\tau_2)$ can be regarded as the approximation of the exact solution $a_0 = a_0(\tau_2)$, and likewise the function $n_0 = \tilde{n}_0(\tau_2)$, $S_0 = \tilde{S}_0(\tau_2)$ and $C_0 = \tilde{C}_0(\tau_2)$ can be regarded as the approximation to the exact solutions $n_0 = n_0(\tau_2)$, $S_0 = S_0(\tau_2)$ and $C_0 = C_0(\tau_2)$, where

$$\tilde{n}_0(\tau_2) = \frac{\beta_{12}(\alpha_1 + \beta_{10}\tilde{a}(\tau_2))}{(e^{-d\tau_2}\theta_1\beta_1 - \beta_{11}\alpha_1) - \beta_{10}\beta_{11}\tilde{a}(\tau_2)},$$

$$\tilde{S}_0(\tau_2) = \frac{\pi_1\alpha_1\tilde{a}(\tau_2) + \pi_2\beta_{10}\tilde{a}^2(\tau_2)}{\delta},$$

$$\tilde{C}_0(\tau_2) = \frac{1}{\alpha_2}[q_c + \lambda_{11}\tilde{a}(\tau_2) - \delta_1\tilde{S}(\tau_2)].$$

The approximate and exact solutions corresponding to the different values of τ_2 have been listed in Table 5. We can see that the errors between them are relatively negligible, and will not affect the following numerical simulation.

With the help of MATLAB, we first identify the feasible region for (ω, τ_2), that is, the two simply connected regions enclosed by the red and blue curves and coordinate axes in Fig. 4, which are marked as Ω_1 and Ω_2. Then the admissible range $I_1 = (0.006, 0.092)$ and $I_2 = (0, 0.081)$

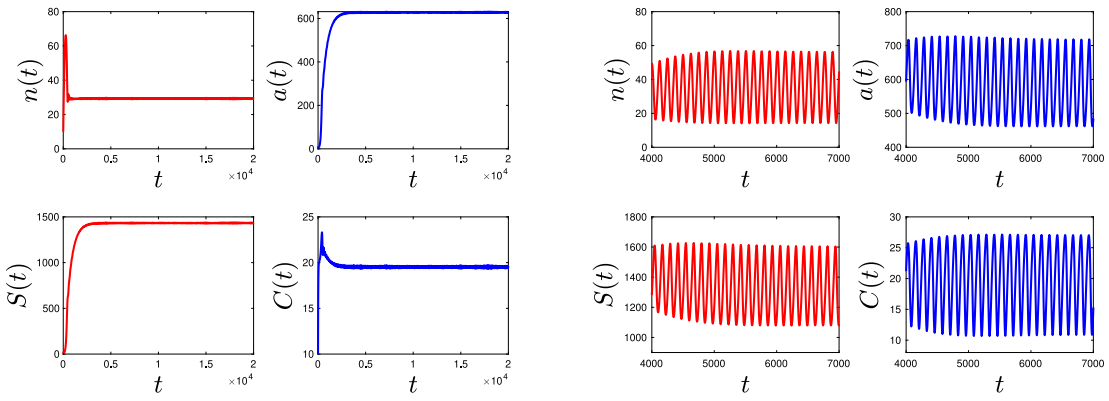

(a) $(\tau_1, \tau_2) = (52, 5)$ (b) $(\tau_1, \tau_2) = (65, 5)$

Fig. 2. (a) E_1 is stable for $(\tau_1, \tau_2) = (52, 5)$; (b) A stable periodic solution is bifurcated from E_1 as τ_1 increases to 65, while E_1 becomes unstable.

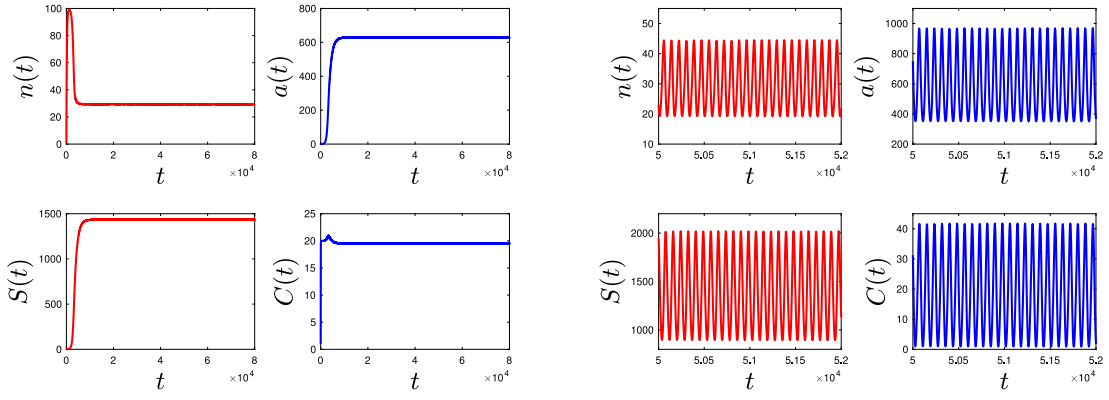

(a) $(\tau_1, \tau_2) = (65, 50)$ (b) $(\tau_1, \tau_2) = (65, 90)$

Fig. 3. (a) E_1 is stable for $(\tau_1, \tau_2) = (65, 50)$; (b) A stable periodic solution is bifurcated from E_1 as τ_2 increases to 90, while E_1 becomes unstable.

Table 5
Comparison of the exact and approximate solutions.

τ_2 (days)	0.1	0.3	0.5	0.7	1	1.2
$a_0 = a_0(\tau_2)$ (mg l^{-1})	567.87	464.08	375.25	295.36	172.83	78.44
$a_0 = \tilde{a}_0(\tau_2)$ (mg l^{-1})	561.71	460.55	373.26	293.31	172.58	78.43
$n_0 = n_0(\tau_2)$ (mg l^{-1})	30.93	34.89	40.13	47.24	63.82	82.00
$n_0 = \tilde{n}_0(\tau_2)$ (mg l^{-1})	30.87	34.85	40.10	47.22	63.81	82.00
$S_0 = S_0(\tau_2)$ (mg l^{-1})	1293.83	1054.95	851.36	666.65	390.37	176.80
$S_0 = \tilde{S}_0(\tau_2)$ (mg l^{-1})	1279.62	1046.85	846.80	664.25	389.80	176.74
$C_0 = C_0(\tau_2)$ (mg l^{-1})	19.72	19.98	20.13	20.21	20.21	20.13
$C_0 = \tilde{C}_0(\tau_2)$ (mg l^{-1})	19.74	19.99	20.13	20.21	20.21	20.13

of ω are obtained. For each $\omega \in I_k$, $k = 1, 2$, the corresponding critical value τ_2 can be found by solving the zeros of the function $S_n^{\pm}(\omega, \tau_2)$. By tracing points, we get the Curve C in Fig. 4. According to formulas (9) and (12), the crossing curves and the crossing directions are shown in Fig. 5.

It can be observed that the crossing curves (i.e. bifurcation curves in Fig. 5) are mainly composed of two families of curves with different shapes. One family is located below the red straight line and contains numerous semicircular curves with openings downward, which correspond to the Curve C in Ω_1, and the other family is located above the red curve and consists of several parabolic curves with openings to the right, which correspond to the Curve C in Ω_2. The red line is $\tau_2 = 1.33$, which is the value that makes $(e^{-d\tau_2}\theta_1\beta_1 - \beta_{11}\alpha_1)q - \beta_{12}\alpha_0\alpha_1 = 0$. A simple analysis shows that the interior positive equilibrium $\mathcal{E}_1(n_0, a_0, S_0, C_0)$ exists only when the (τ_1, τ_2) value are below the red line, that is, $\tau_2 < 1.33$.

Comparing Figs. 1 and 5, we find that the crossing curves between the degenerate model and the non-degenerate model are quite different, and these differences still exist even if the value of τ_2 is very small. In a biological sense, these differences can result in distinct suggestions for the advancement of fisheries. Here we make a detailed analysis as follows:

(1) From Fig. 5, it can be seen that when $\tau_2 = 0$ in the non-degenerate model, the first critical value of the detritus-nutrient recycling delay $\tau_1 \approx 42.12$, basically consistent with the result of the degenerate model, with an error of about 0.12 days. This slight error is caused by the approximation of the equilibrium point during the numerical simulation.
(2) The degenerate model has no restriction on the value of τ_2 because the existence of the internal equilibrium point of the model is independent of τ_2. However, if we consider the mortality

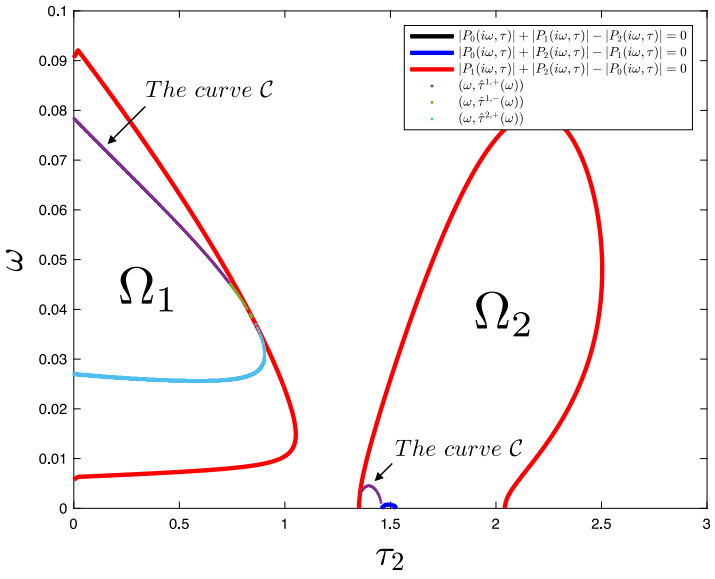

Fig. 4. The Curve $\mathcal{C}$.

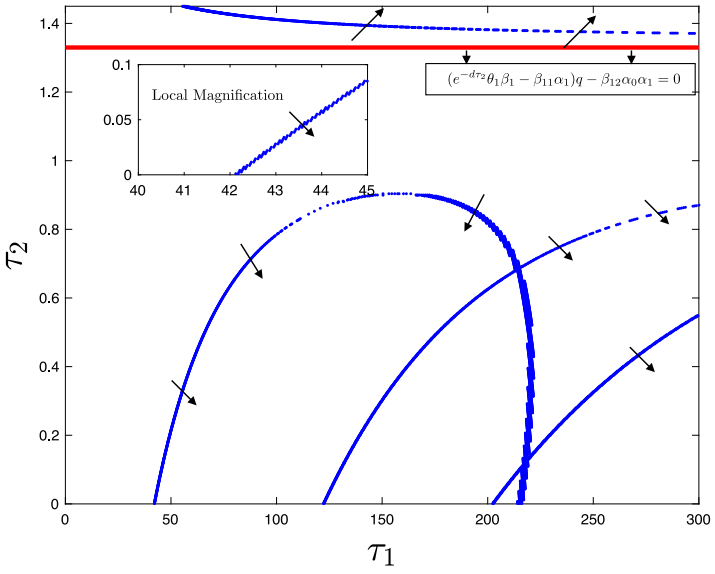

Fig. 5. Crossing curves and crossing directions.

of algae in the process of absorbing and digesting nutrients, the situation is completely different. In the non-degenerate model, we can see that (i) when $\tau_2 > 1.33$, the internal equilibrium point $\mathcal{E}_1$ does not exist, and there is only one boundary equilibrium point $\mathcal{E}_0(q/\alpha_0, 0, 0, q_c/\alpha_2)$ in the system. The numerical simulation results show that this trivial equilibrium point is always stable (see Fig. 6). The results suggest that when it takes too long for nutrients to be converted into the energy needed for algae to grow, the algae will eventually die out due to the death phenomenon present in the process. (ii) When $0.91 < \tau_2 < 1.33$, the internal equilibrium point $\mathcal{E}_1$ is always stable, and this dynamic behavior will not change with the increase of τ_1, see Fig. 6. That is to say, when the energy conversion time τ_2 is in a suitable interval, the whole water body will be in a very stable state. In particular, the density of algae and fish will be maintained at a certain level without fluctuation. (iii) When $\tau_2 < 0.91$, the stability of $\mathcal{E}_1$ will be affected by τ_1. In more detail, it can be seen from the bifurcation diagram that as τ_1 increases from zero and passes through the first crossing curve, $\mathcal{E}_1$ will change from stable to unstable, and at the same time, a stable periodic solution will be bifurcated from $\mathcal{E}_1$, Fig. 7 validates this result. This means that when the time for nutrient conversion to algae growth is relatively short, and the time for the cycle from detritus to nutrients is too long, the water ecosystem will oscillate, causing a sharp decline in fish density and damaging the economic interests of fishermen. Therefore, in order to avoid such oscillations, we can regularly clean up detritus in the lake to ensure the stability of the water system.

(3) We would like to give a new suggestion on the time window to remove detritus from the lake. Considering the cost of personnel and tools, this time window should not be too frequent, and considering the stability of the entire water ecosystem, this cleaning period should not be too long. It can be seen from the analysis that this time window must be longer than the 42 days mentioned in Misra et al. (2011), and it is positively correlated with τ_2, which is similar to the result of the degenerate model, but the suggested value is still greater than that of the degenerate model. More specifically, for both degenerate and non-degenerate models, the critical crossing curve can be approximated as a straight line

Table 6
Time window for removal of detritus in a lake.

Value of τ_2 (days)	0.2	0.4	0.6	0.8
Suggestions from the degenerate model (days)	42	43	43.5	44
Suggestions from the non-degenerate model (days)	49	59	73	104

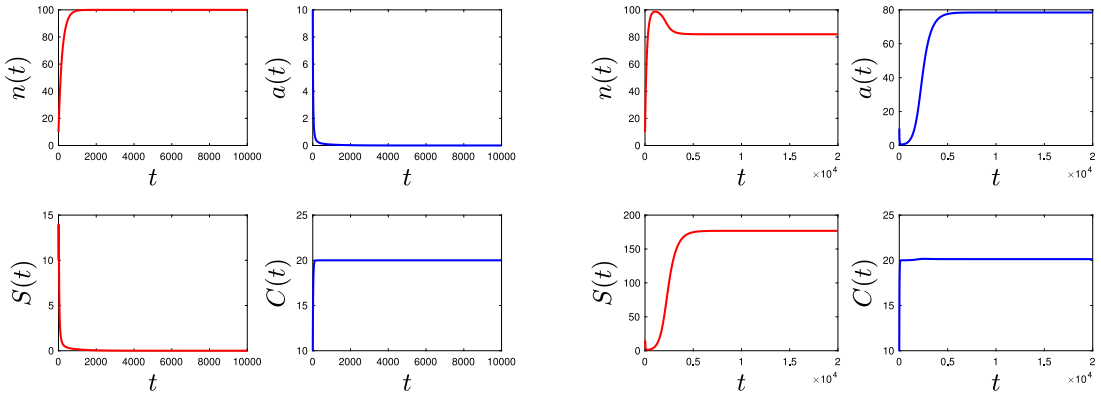

(a) $(\tau_1, \tau_2) = (100, 1.4)$ (b) $(\tau_1, \tau_2) = (100, 1.2)$

Fig. 6. (a) $\mathcal{E}_0$ is stable for $\tau_2 > 1.3$; (b) $\mathcal{E}_1$ is stable for $0.91 < \tau_2 < 1.3$.

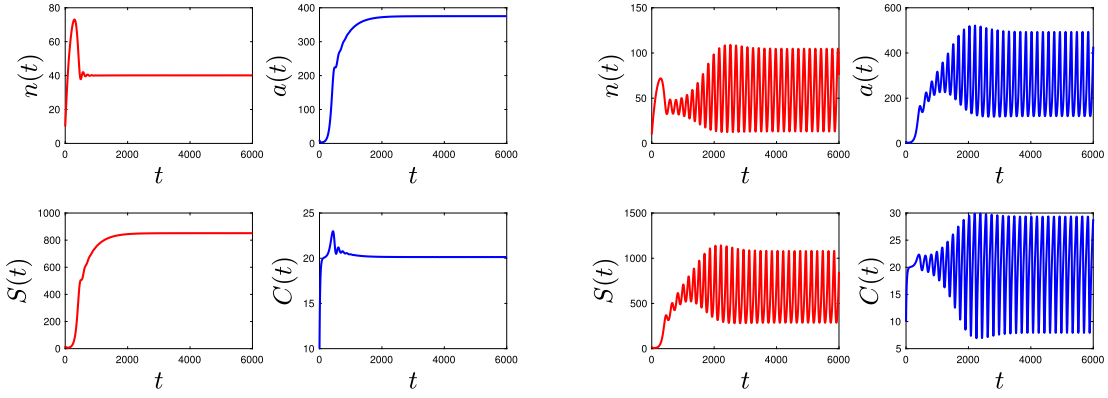

(a) $(\tau_1, \tau_2) = (50, 0.5)$ (b) $(\tau_1, \tau_2) = (100, 0.5)$

Fig. 7. (a) $\mathcal{E}_1$ is stable for $(\tau_1, \tau_2) = (50, 0.5)$; (b) A stable periodic solution is bifurcated from $\mathcal{E}_1$ as τ_1 increases to 100, while $\mathcal{E}_1$ becomes unstable.

when τ_1 and τ_2 are small, as shown in the partial enlarged view in Figs. 1 and 5. The slope of the line corresponding to the degenerate model is greater than that of the line corresponding to the non-degenerate model, so the recommended number of days given by the non-degenerate model will be greater than that given by the degenerate model. See Table 6 for the relevant values. The results in Table 6 are reasonable because in the non-degenerate model we considered algal death during the absorption and digestion of nutrients. Then under the same conditions it is expected that algal bloom should be less serious predicted by the non-degenerate model. As a result, the control time window can be longer for the non-degenerate model.

5. Discussion

In this paper, we proposed and analyzed a class of algal growth models with algal digestion delay and detritus-nutrient recycling delay, and considered two different scenarios, namely, the presence and absence of algal death during nutrient absorption. Among them, the degenerate model ignores mortality rate of algae during the absorption and digestion of nutrients, while the non-degenerate model considers the survival rate of algae during the reproductive process. Mathematically, they are fundamentally different. The non-degenerate model is a system of functional differential equations with coefficients dependent on algal digestion delay τ_2, which is more difficult to study.

The degenerate model demonstrates that eutrophication in water bodies contributes to an increase in algae abundance and a decline in dissolved oxygen concentration, thereby posing detrimental effects on ecological integrity and fishery development. Consequently, it holds immense importance to mitigate the direct discharge of agricultural and industrial wastewater. Furthermore, we aim to establish a timeframe for detritus removal from the lake. Upon analyzing the two models, we observe that the non-degenerate model suggests a considerably longer recommended timeframe compared to the degenerate model. Additionally, the suggested timeframe in the degenerate model slightly exceeds that of the model without considering algal digestion delay (i.e., 42 days). This indicates an underestimation of the required time window, leading to potential waste of personnel and resources.

From the biological point of view, the non-degenerate model seems more reasonable. For the non-degenerate model, the unique internal equilibrium exists only when τ_2 is less than a certain threshold (i.e., $\tau_2 < 1.33$), and when τ_2 is greater than this threshold, the algae

will become extinct. The degenerate model has no such limitation and is more similar to the model without algal digestion delay.

We have also discovered some rich dynamic phenomena. Both of these two models exhibit stability switching of equilibrium points, but there are noticeable differences in the critical parameters that trigger these transitions. For the degenerate model, when τ_1 is fixed, increasing the value of τ_2 can cause the positive equilibrium to switch from stability to instability and back to stability. This switching behavior can occur infinitely, distinguishing it from the model without algal digestion delay. In contrast, for the non-degenerate model, the key parameter driving stability switching of the equilibrium point is τ_1. Furthermore, we had an intriguing observation for the non-degenerate model where there is a safe zone. When τ_2 is within a suitable range (i.e., $0.91 < \tau_2 < 1.33$), the internal equilibrium point remains stable, rendering the system unaffected by the detritus-nutrient recycling delay τ_1. In this case, the density of algae and fish remains within a stable range, preventing algal blooms and facilitating ongoing fishery development. This novel finding distinguishes our model from previous ones and contributes to our understanding of the system dynamics.

CRediT authorship contribution statement

Qi An: Formal analysis, Funding acquisition, Investigation, Methodology, Software, Visualization, Writing – original draft. **Hao Wang:** Conceptualization, Funding acquisition, Investigation, Methodology, Supervision, Writing – review & editing, Resources. **Xiunan Wang:** Conceptualization, Investigation, Methodology, Project administration, Supervision, Writing – review & editing.

Declaration of competing interest

The authors declare that they have no known competing financial interests or personal relationships that could have appeared to influence the work reported in this paper.

Data availability

No data was used for the research described in the article.

Acknowledgments

Research of QA is partially supported by National Natural Science Foundation of China 12101318, Natural Science Found of Jiangsu Province BK2020080 and Natural Science Fund Project of Colleges in Jiangsu Province 20KJB110009. Research of HW is partially supported by the Natural Sciences and Engineering Research Council of Canada (Individual Discovery Grant RGPIN-2020-03911 and Discovery Accelerator Supplement Award RGPAS-2020-00090) and the Canada Research Chair program (Tier 1 Canada Research Chair Award).

References

Alam, M.Z., Otaki, Furumai, H., Ohgaki, S., 2001. Direct and indirect inactivation of microcystis aeruginosa by uv-radiation. Water Res. 35 (4), 1008–1014.

Amemiyaa, T., Enomotoa, T., Rossberga, A.G., Yamamotob, T., Inamoric, Y., Itoha, K., 2007. Stability and dynamical behavior in a lake-model and implications for regime shifts in real lakes. Ecol Model 206, 54–62.

An, Q., Beretta, E., Kuang, Y., Wang, C., Wang, H., 2019. Geometric stability switch criteria in delay differential equations with two delays and delay dependent parameters. J. Differ. Equ. 266 (11), 7073–7100.

Anderson, D.M., 2009. Approaches to monitoring, control and management of harmful algal blooms (habs). Ocean Coastal Manag. 52 (7), 342–347.

Balaji-Prasath, B., Wang, Y., Su, Y.P., Hamilton, D.P., Lin, H., Zheng, L., Zhang, Y., 2022. Methods to control harmful algal blooms: a review. Environ. Chem. Lett. 20 (5), 3133–3152.

Berdalet, E., Fleming, L.E., Gowen, R., Davidson, K., Hess, P., Backer, L.C., Moore, S.K., Hoagland, P., Enevoldsen, H., 2016. Marine harmful algal blooms, human health and wellbeing: challenges and opportunities in the 21st century. J. Marine Biol. Assoc. United Kingdom 96 (1), 61–91.

Chattopadhyay, J., Sarkar, R.R., el Abdllaoui, A., 2002. A delay differential equation model on harmful algal blooms in the presence of toxic substances. Math. Med. Biol. J. IMA 19 (2), 137–161.

Chen, M., Fan, M., Liu, R., Wang, X., Yuan, X., Zhu, H., 2015. The dynamics of temperature and light on the growth of phytoplankton. J. Theoret. Biol. 385, 8–19.

Chen, F., Li, Z., Chen, X., Laitochová, J., 2007. Dynamic behaviors of a delay differential equation model of plankton allelopathy. J. Comput. Appl. Math. 206 (2), 733–754.

Christian, B., Luckas, B., 2008. Determination of marine biotoxins relevant for regulations: from the mouse bioassay to coupled lc-ms methods. Anal. Bioanal. Chem. 391, 117–134.

Conley, D.J., Paerl, H.W., Howarth, R.W., Boesch, D.F., Seitzinger, S.P., Havens, K.E., Lancelot, C., Likens, G.E., 2009. Controlling eutrophication: nitrogen and phosphorus.

Dehghani, M.H., 2016. Removal of cyanobacterial and algal cells from water by ultrasonic waves—a review. J. Molecular Liquids 222, 1109–1114.

Ebenezer, V., Lim, W., Ki, J.S., 2014. Effects of the algicides cuso 4 and naocl on various physiological parameters in the harmful dinoflagellate cochlodinium polykrikoides. J. Appl. Phycol. 26, 2357–2365.

Grattan, L.M., Holobaugh, S., Morris, Jr., J.G., 2016. Harmful algal blooms and public health. Harmful Algae 57, 2–8.

Gu, K., Niculescu, S., Chen, J., 2005. On stability crossing curves for general systems with two delays. J. Math. Anal. Appl. 311 (1), 231–253.

Huppert, A., Blasius, B., Olinky, R., Stone, L., 2005a. A model for seasonal phytoplankton blooms. J. Theoret. Biol. 236 (3), 276–290.

Huppert, A., Blasius, B., Olinky, R., Stone, L., 2005b. A model for seasonal phytoplankton blooms. J. Theoret. Biol. 236 (3), 276–290.

Jeppesen, E., Mehner, T., Winfield, I.J., Kangur, K., Sarvala, J., Gerdeaux, D., Rask, M., Malmquist, H.J., Holmgren, K., Volta, P., et al., 2012. Impacts of climate warming on the long-term dynamics of key fish species in 24 European lakes. Hydrobiologia 694, 1–39.

Jøorgensen, Sven Erik, 1976. A eutrophication model for a lake. Ecol. Model. 2 (2), 147–165.

Kent, M.L., Whyte, J.N.C., LaTrace, C., 1995. Gill lesions and mortality in seawater pen-reared atlantic salmon salmo salar associated with a dense bloom of skeletonema costatum and thalassiosira species. Dis. Aqua. Organ. 22 (1), 77–81.

Lin, X., Wang, H., 2012. Stability analysis of delay equations with two discrete delays. Can. Appl. Math. Q. 20 (4), 519–533.

Misra, A.K., Chandra, P., Raghavendra, V., 2011. Modeling the depletion of dissolved oxygen in a lake due to algal bloom: Effect of time delay. Adv. Water Resour. 34, 1232–1238.

Mukhopadhyay, A., Chattopadhyay, J., Tapaswi, P.K., 1998. A delay differential equations model of plankton allelopathy. Math. Biosci. 149 (2), 167–189.

O'Brien, W.J., 1974. The dynamics of nutrient limitation of phytoplankton algae: a model reconsidered. Ecology 55 (1), 135–141.

Sabater, S., 2009. Diatoms. Encyclopedia of Inland waters. pp. 149–156.

Sanseverino, I., Conduto, D., Pozzoli, L., Dobricic, S., Lettieri, T., et al., 2016. Algal Bloom and Its Economic Impact. European Commission. Joint Research Centre Institute for Environment and Sustainability.

Sellner, K.G., Doucette, G.J., Kirkpatrick, G.J., 2003. Harmful algal blooms: causes, impacts and detection. J. Ind. Microbiol. Biotechnol. 30, 383–406.

Shukla, J.B., Misra, A.K., Chandra, Peeyush, 2008. Modeling and analysis of the algal bloom in a lake caused by discharge of nutrients. Appl. Math. Comput. 196 (2), 782–790.

Voinov, A.A., Tonkikh, A.P., 1987. Qualitative model of eutrophication in macrophyte lakes. Ecol. Model. 35 (3), 211–226.

Wang, X., Wang, H., Li, M.Y., 2019. R_0 and sensitivity analysis of a predator–prey model with seasonality and maturation delay. Math. Biosci. 315, 108225.

William, M., Lewis, J., Wurtsbaugh, W.A., 2008. Control of lacustrine phytoplankton by nutrients: erosion of the phosphorus paradigm. Int. Review Hydrobiol. 93 (4–5), 446–465.

Wong, Ken T.M., Lee, Joseph H.W., Hodgkiss, I.J., 2007. A simple model for forecast of coastal algal blooms. Estuar. Coast. Shelf Sci. 74 (1–2), 175–196.

Xiao, X., Li, C., Huang, H., Lee, Y., 2019. Inhibition effect of natural flavonoids on red tide alga phaeocystis globosa and its quantitative structure–activity relationship. Environ. Sci. Pollut. Res. 26, 23763–23776.

Zachleder, V., Bišová, K., Vítová, M., 2016. The cell cycle of microalgae. Physiol. Microalgae 3–46.

Zhang, F., Ye, Q., Chen, Q., Yang, K., Zhang, D., Chen, Z., Lu, S., Shao, X., Fan, Y., Yao, L., et al., 2018. Algicidal activity of novel marine bacterium paracoccus sp. strain y42 against a harmful algal-bloom-causing dinoflagellate, prorocentrum donghaiense. Appl. Environ. Microbiol. 84 (19), e01015–18.

Zhao, S., Yuan, S., Wang, H., 2020. Threshold behavior in a stochastic algal growth model with stoichiometric constraints and seasonal variation. J. Differential Equations 268 (9), 5113–5139.